
# LCLS-II Beam and FEL Performance Based on Start-to-End Simulations Using a Gaussian-profile injector Laser

LCLS-II-TN-20-03

6/5/20

N. Neveu, N. Sudar, Y. Ding*, G. Marcus, A. Marinelli, C. Mayes

SLAC, Menlo Park, CA 94025, USA

J. Qiang

LBNL, Berkeley, CA 94720, USA

*ding@slac.stanford.edu

## *Abstract:*

In this technical note we evaluate the beam and FEL performance for LCLS-II starting from a laser with a Gaussian-shape temporal profile in the gun, as measured during the Early Injector Commissioning. We choose the bunch charge of 100 pC as a baseline, and also briefly discussed the 50 pC case. The injector area was optimized with Astra, followed with Elegant simulations in the linac, compressors, and transport line, and finally used Genesis for the FEL simulations. One configuration has been benchmarked with IMPACT simulations using real number of particles.


# 1 Introduction

In the LCLS-II, start-to-end simulations play an important role for system design and performance evaluation. In the previous LCLS-II simulations, the injector laser was based on a flat-top temporal profile and the beam and FEL simulations are summarized in this technical note [1]. During the Early Injector Commissioning (EIC), the injector laser temporal profile has a Gaussian shape. Although laser shaping to get a flat-top shape is under development, we are preparing to continue with the similar Gaussian-profile laser during the LCLS-II linac and FEL commissioning. It is interesting and also important to evaluate the beam and FEL performance with such a laser. We recently performed simulations using 100-pC and 50-pC bunch, and in this technical note we summarize the machine configuration and beam/FEL performance based on the Gaussian shape laser.

# 2 100-pC Injector simulations with Astra

The input UV laser distribution used in the following Astra [2] simulations has a full width half maximum (FWHM) of 20 picoseconds (ps), based on measurements by the laser group. As mentioned above this varies from the flattop distribution used for LCLS-II design work [1]. We show in Figure 1 of the laser temporal profiles being used in simulations, and one example of the measurement during EIC commissioning.

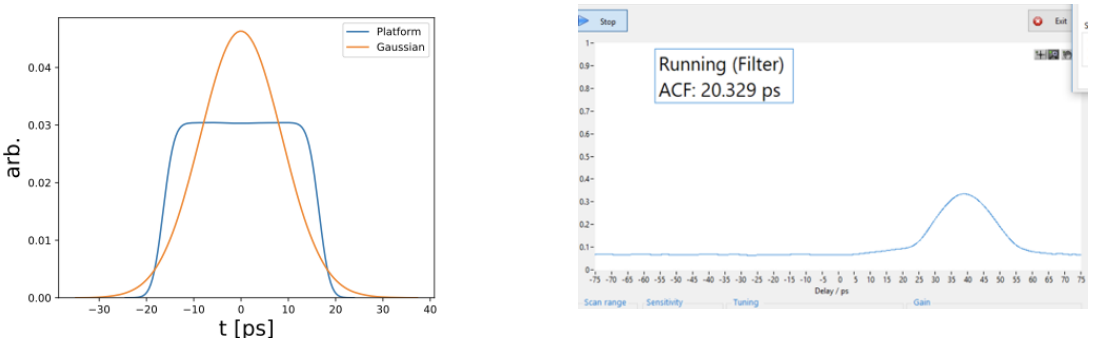


**Figure 1: The UV laser temporal profiles used in simulations (left, flat-top and gaussian shape), and one measurement example (right). Measurement was performed by S. Gilevich, A. Miahnarhri, and S. Droste using a cross-correlator.**

The simulation for the injector is based on the current LCLS-II design and operation specifications. This includes the gun, solenoids, and the first cryomodule, which ends at about 14 meters with final beam energy about 100 MeV.

Optimization of variable parameters is performed to minimize emittance and bunch length. Currently this is done using a Generic algorithm (NSGA-II) [3, 4] with many simulations on the SLAC or NERSC clusters. The results are viewed on a Pareto front, i.e. plotting emittance and bunch length for each simulation. This gives a relative tradeoff between the two values. For example, when the emittance is small, the bunch length is likely to be large, and vice versa due to space charge forces. Based on work by others (C. Mitchell, J. Qiang, F. Zhou et al.), it is also known that the emittance values for a Gaussian profile will be larger than that of a flattop, for a given set of parameters. The absolute difference in performance when optimization is allowed is not yet know (i.e. allowing different settings in the Gaussian case can improve performance to some degree).

During the injector optimization, some of the parameters are set constant, based on experience and early optimization results. In the following Table 1 we list the settings for a few constant parameters (Note: constants in Table 1 were taken from previous simulation runs by F. Zhou and C. Mitchell), while in Table 2 it shows the variable parameters in the optimization, including the range and the optimal settings we chose for next step. The bunch charge is 100 pC and the final energy out of the firs cryomodule is set to be no less than 90 MeV. Thermal emittance is set with MTE 250 meV here (effectively thermal emittance slope is 0.7 um/mm).

**Table 1: Constant parameters for injector optimizations**

| Parameter | Value | Unit |
|---|---|---|
| **Gradient on cathode** | 20 | MV/m |
| **Gradient in buncher** | 1.79 | MV/m |
| **Cavity peak field*: Cavity 5-8** | 32 | MV/m |
| **Cavity phase: Cavity 5-8:** | 0, 0, 1.25, 6 | deg |

**Table 2: Variable parameters for injector optimizations with 100-pC, and one optimized solution.**

| Parameters | Min | Max | Unit | Selected operating point |
|---|---|---|---|---|
| **Laser radius** | 0.15 | 0.75 | mm | 0.5 |
| **Laser FWHM** | 1.0 | 40 | ps | 20 |
| **Gun phase** | -10 | 10 | deg | 6 |
| **Buncher phase** | -90 | -40 | deg | -85 |
| **Solenoid 1 and 2** | 0.0 | 0.075 | T | 0.0545, 0.0285 |
| **Cavity peak field*: Cavity 1-4** | 0.0 | 32 | MV/m | 12, 3, 18, 7 |
| **Cavity phase: Cavity 1-4** | -20 | 20 | deg | -2, -20, 3, -10 |
| ***: *note the peak field of the SC cavity is 1.9 times the average gradient, i.e., peak field here 32 MV/m* | | | | |

*means average gradient 16.8 MV/m.*

The optimization runs were done using code from [5], and lattice files can be found here [6, 7]. In the Figure 2 example using Astra code the laser variables were held constant at 0.5 mm radius and 20 ps fwhm temporal although in general these can be optimized as listed in Table 2. As a starting point for gauging downstream performance, one point with bunch duration of 1 mm at the Pareto front curve was chosen. For the chosen operating point (parameters listed in Table 1 and Table 2), we show the emittance and bunch length evolution in Figure 3. We see the bunch length is 1 mm with 95% emittance about 0.33 um. In Figure 4 we show the final beam longitudinal phase space and current profile at the exit of the first cryomodule. The beam energy is about 92 MeV. This beam will be used for next step tracking.

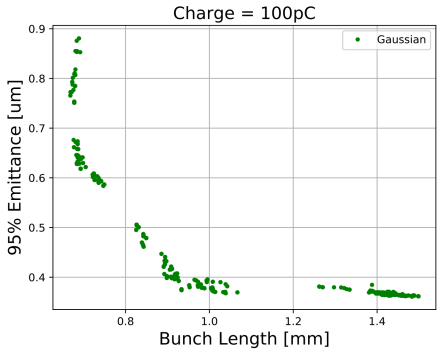


**Figure 2: One example of the Pareto front for system optimization using the Gaussian shape laser. The parameters used for optimization are shown in Table 1 and Table 2. In this example, the laser radius (0.5 mm) and length (20 ps) were fixed.**

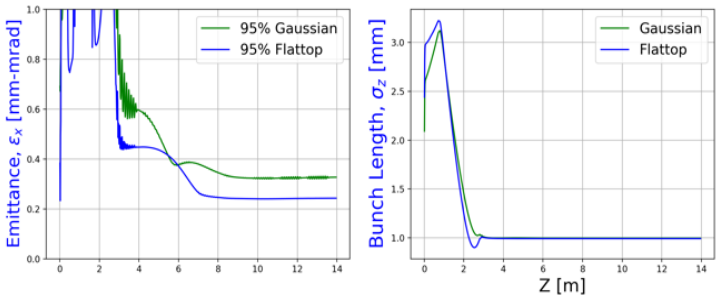


**Figure 3: Emittance and bunch length evolution in the injector Astra simulations for the chosen operating point.**

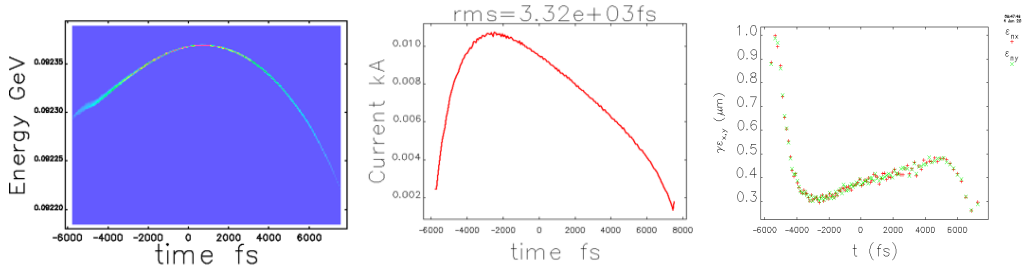


**Figure 4: Longitudinal phase space, current profile, and slice emittance at the exit of the injector for the chosen operating point from Astra simulations. Bunch charge is 100 pC, bunch head is to the left.**

# 3 Linac Configuration-1: "V" shape electron beam

For the Linac and transport lines, we used Elegant code [8] with 10 million macroparticles generated from Astra simulations as shown in Section 2. The configuration was first optimized using LiTrack [9] to generate a reasonable final longitudinal phase space and current profile with considering the available cavity voltage in each section and the chicane R56 range. Then we set up the Elegant based on optimized LiTrack configuration to include the CSR, longitudinal space charge and also transverse dynamics.

The one linac and chicane configuration for the 100-pC bunch charge are shown in the following Table-3.

**Table 3: Linac and chicane configuration-1 for 100 pC bunch.**

| parameters | value | unit |
|---|---|---|
| Injector beam E. | 92 | MeV |
| Bunch charge | 100 | pC |
| Laser heater | 7 | keV |
| L1 amplitude | 14.0625*16 | MV |
| L1 phase | -25 | deg |
| L1H phase | -158 | deg |
| L1H Amp. | 50 | MV |
| BC1 Energy | 250 | MeV |
| BC1 R56 | -45 | mm |
| L2 amplitude | 15.8533*96 | MV |
| L2 phase | -27.5 | deg |
| BC2 energy | 1600 | MeV |
| BC2 R56 | -43 | mm |
| L3 amplitude | 15*160 | MV |
| L3 phase | 0 | deg |
| final energy | 4000 | MeV |

The two beamlines starting the spreader area to hard x-ray undulator and soft x-ray undulator are tracked separately. The final phase space and current profile at the entrance of each undulator is very similar. Here we show one example at the entrance of the hard x-ray undulator in Figure 4. We see the longitudinal phase space has a "V" shape, and the bottom part has the highest current over 1kA. This "V" shape beam is not ideal for generating narrow bandwidth SASE, and the bunch head chirp is mainly from longitudinal space charge. However, we think it is a useful distribution to generate relatively short x-ray pulse by selective lasing on the core part with a post-saturation taper, or apply a chirp-taper scheme to have two-color x-ray FELs.

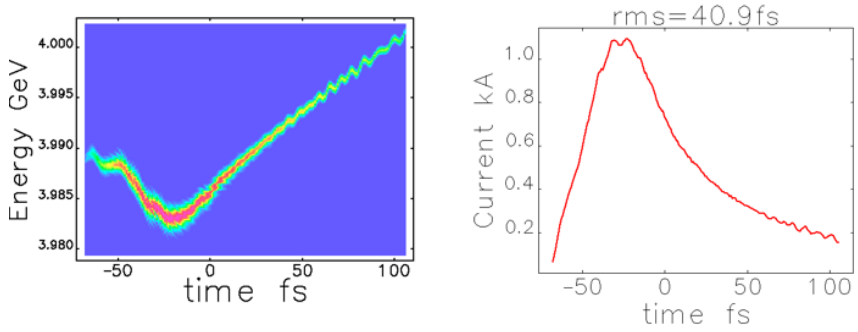


**Figure 4: Final longitudinal phase space and current profile at the entrance of the hard x-ray undulator from configuration-1. Bunch charge is 100 pC, head to the left.**

For the FEL simulations, we used Genesis code [10] and chose one photon energy for each undulator line for a demonstration: 1.25 keV for soft x-ray and 3.25 keV for hard x-ray. We used all the undulator segment in each setup but without applying post saturation tapter, that is, the undulator K is kept constant even after reaching saturation. The electron beam at the entrance of the undulator was matched as a whole bunch, without purposely matching the core part of the beam.

The exemplary FEL power profile at the end of each undulator line are shown in Figure 5. At the saturation point (see gain curve in Figure 6), actually both x-ray pulses are relatively short, lasing mainly at the core high current section. After saturation, the low current part of the bunch also has made a pretty good lasing through the whole undulator, which makes both the power profiles in Figure 5 have a tail-like distribution. The 3.25keV case even looks like having two pulses. We believe if we apply a proper post-saturation taper after core part saturation, the high current core part lasing will be continued which could maintain the x-ray pulse relatively short.

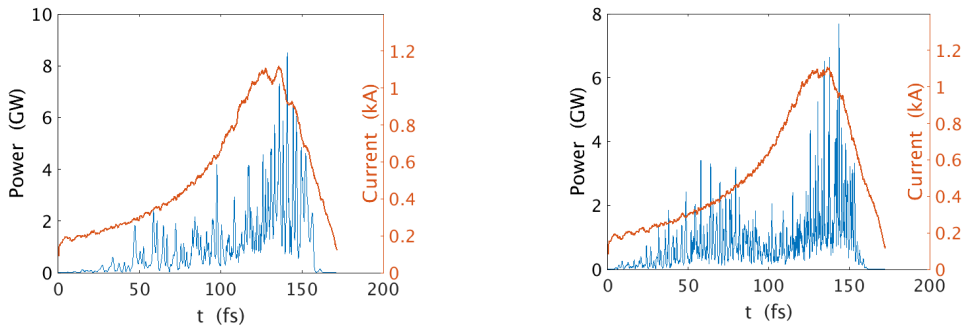


**Figure 5: The FEL power profile at the end of the undulator line for 1.25 keV (left) and 3.25 keV (right) using beam in Figure 4. The head is to the right. No post saturation taper has been applied.**

To compare with the previous results which used a flat-top laser profile in [1], we plotted the FEL gain curves of the same photon energy, from a flat-top laser and a Gaussian laser, respectively. Note in previous flat-top simulations [1] the linac and transport line parts are tracked with IMPACT code [11, 12] using real number particles including 3-D space charge forces. For this Gaussian laser case, we tracked the beam with 10 million macroparticles using Astra and Elegant which could underestimate some collective effects. There is no taper being applied after saturation in all our simulation examples here. We plot the gain curves in Figure 6. We can see that the number of photons is a bit less for the Gaussian laser case, but the gain is higher and saturation length is shorter. The shorter gain length mainly benefits from a higher current in the Gaussian laser case (the flat-top laser beam in [1] has a current about 800 A). At the same time, for the Gaussian laser case the pulse duration is also shorter, and the peak power is actually similar to the flattop laser case.

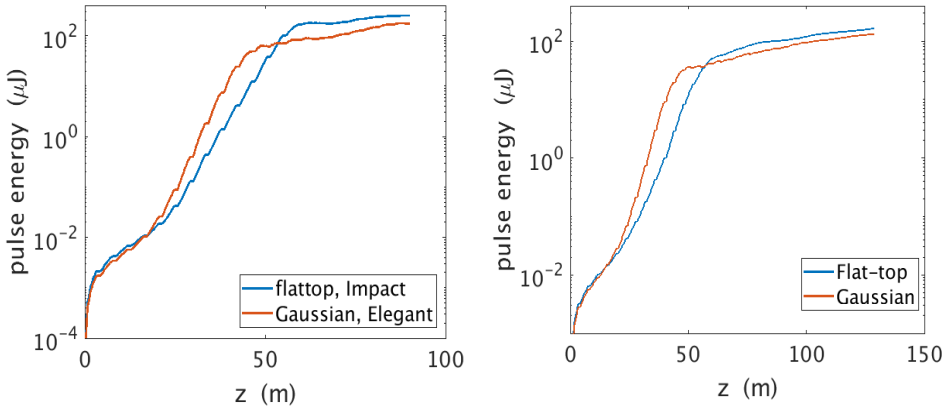


**Figure 6: FEL gain curves with the "V" shape beam at 1.25 keV (left) and 3.25 keV (right). No post-saturation taper is used.**

# 4 Linac Configuration-2: "L" shape phase space and IMPACT benchmark

## 4.1 Elegant tracking with Astra output beam

In the LCLS-II, due to the ~2-km long bypass line, longitudinal space charge (LSC) force plays an important role affecting the final phase space. Another configuration has been optimized with achieving a smaller current ramp at the bunch head which helps reduce the LSC force. This leads to a flat chirp at the bunch head and core, forming a "L" shape instead of the previous "V" shape of the longitudinal phase space. The BC2 energy is reduced to 1.5 GeV at this setup but the final energy is still 4 GeV. The optimized linac configuration is listed in Table 4.

Based on the configuration in Table 4, we performed Elegant tracking show one example of the beam longitudinal phase space and current profile at the entrance of the hard x-ray undulator entrance in the following Figure 7. We see in this example, the longitudinal phase space has a flat chirp with most of the

bunch, which could be useful for selfseeding mode or help reduce the SASE bandwidth.

**Table 4: Configuration-2 for 100 pC bunch with BC2 energy at 1500 MeV.**

| parameters | value | unit |
|---|---|---|
| Injector beam E. | 92 | MeV |
| Bunch charge | 100 | pC |
| Laser heater | 7 | keV |
| L1 amplitude | 15*16 | MV |
| L1 phase | -24.9 | deg |
| L1H phase | -173 | deg |
| L1H Amp. | 60 | MV |
| BC1 Eenergy | 250 | MeV |
| BC1 R56 | -53 | mm |
| L2 amplitude | 15.868*96 | MV |
| L2 phase | -34.8 | deg |
| BC2 energy | **1500** | MeV |
| BC2 R56 | -41.5 | mm |
| L3 amplitude | 15.625*160 | MV |
| L3 phase | 0 | deg |
| final energy | 4000 | MeV |

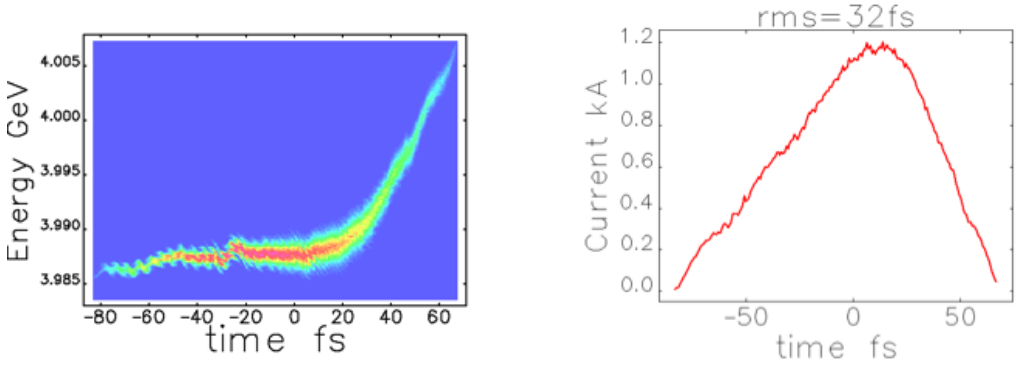


**Figure 7: Elegant simulated final electron beam "L" shape longitudinal phase space and current profile at hard x-ray undulator entrance using configuration-2 in Table 4. Bunch charge is 100 pC with head to the left.**

## 4.2 IMPACT tracking with a Gaussian shape laser

One concern of the tracking results from Elegant is the accuracy of the microbunching effect. In the past, IMPACT code was adopted with the real number of particles to minimize the numerical noise problem. As seen in Figure 4 and Figure 7, we can see some modulation in the head or tail and not sure it is real or from numerical noise. Based on the injector setting as listed in Table 1 and 2, and the linac configuration-2 in Table 4, we run IMPACT simulations with the real number of electrons for benchmarking the Elegant results.

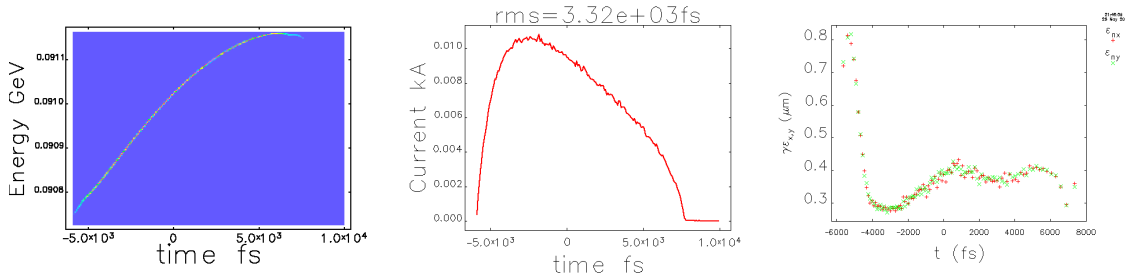


**Figure 8: Electron beam longitudinal phase space, current profile and the slice emittance at the injector exist, from IMPACT simulations with real number of electrons. Bunch charge is 100 pC with head to the left.**

We show the electron beam at the injector exit and at the hard x-ray undulator entrance from IMPACT simulations in Figure 8 and Figure 9. Comparing to the parameters listed in Table 4, BC2 chicane R56 has been changed to -39.7 mm to make a similar current level as we got from Elegant. We believe the reason for this adjustment is mainly due to the beam generated in the injector area from IMPACT-T has a slightly different chirp as that generated from Astra (Figure 4 vs Figure 8). We tested that using the IMPACT-T injector beam and run Elegant tracking, we achieved a very similar final beam between Elegant and IMPACT-Z using the same linac and chicane configuration. Note in Figure 9 the peak current, ~1.4kA, is still slightly higher than that from Astra and Elegant simulations as shown in Figure 7 (~1.2kA). In terms of the purpose for checking the microbunching instability, we see the IMPACT results with real number of particles has a much smoother phase space and current profile. This verifies that the microstructure modulations in the Elegant results are mostly from the numerical noise, but the general features of the electron beam simulated from Elegant such as the current, phase space, and energy chirp are still valid.

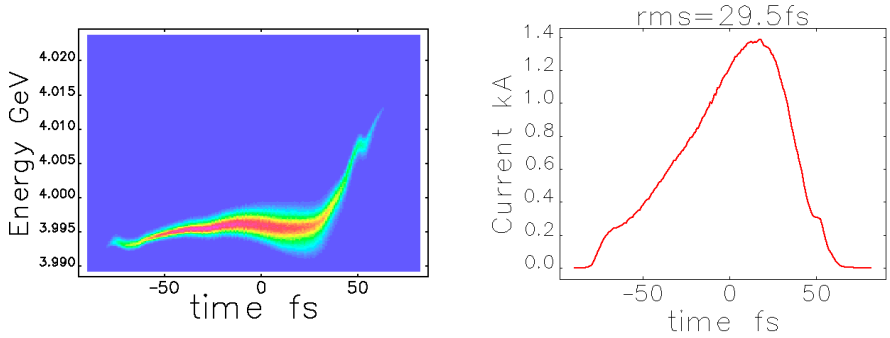


**Figure 9: Electron beam longitudinal phase space and current profile at the HXR undulator entrance from IMPACT simulations with real number of electrons. Bunch charge is 100 pC with head to the left.**

We also plotted the slice emittance and mismatching (BMAG) in Figure 10 for the beam shown in Figure 9. The vertical emittance has a larger variation than the horizontal one, and can be further checked and possibly be improved by correcting some mismathcing issues along the beamline.

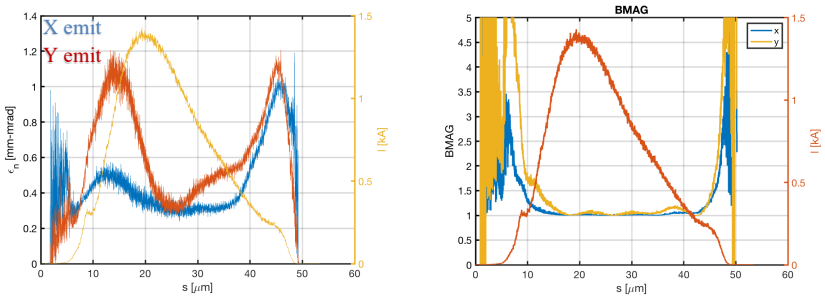


**Figure 10: The slice emittance and mismatching BMAG of the beam (see Figure 9) from IMPACT simulations with the real number of particles. Head is to the right.**

# 4.3 HXR (3.25 keV) FEL simulations with Genesis

Based on "L" shape electron beams generated either from the Astra + Elegant simulations, or form IMPACT simulations, we run Genesis to evaluate the FEL performance.

The FEL photon energy was chosen at 3.25 keV for hard x-ray case in our simulation examples. The hard x-ray undulator period is 2.6 cm, with K=1.265 for this photon energy. We did not include a post-saturation taper of the undulator in our simulation examples, which typically could help double or triple the final number of photons.

We compare the simulated FEL results base on Gaussian shape injector laser from the Astra + Elegant simulations (beam in Figure 7), from the IMPACT simulations (beam in Figure 9), and the flat-top injector laser from IMPACT simulations in 2016 (beam see Ref. [1], ~800 A). The FEL power profiles and spectra at the end of the hard x-ray undulator are shown in Figures 11 and 12.

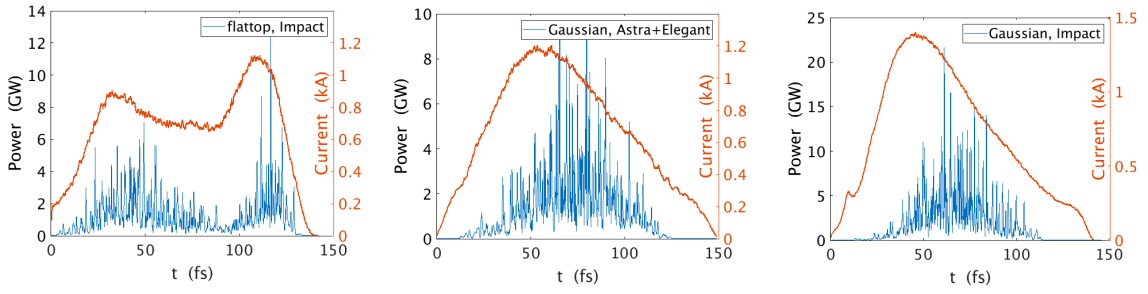


**Figure 11: FEL power profiles at the end of the hard x-ray undulator, at 3.25 keV. Left: flattop injector laser with beam simulated using IMPACT in Ref [1]; middle: Gaussian shape injector laser with beam simulated using Astra + Elegant; Right: Gaussian injector laser with beam simulated using IMPACT. No taper is applied. The head is to the right.**

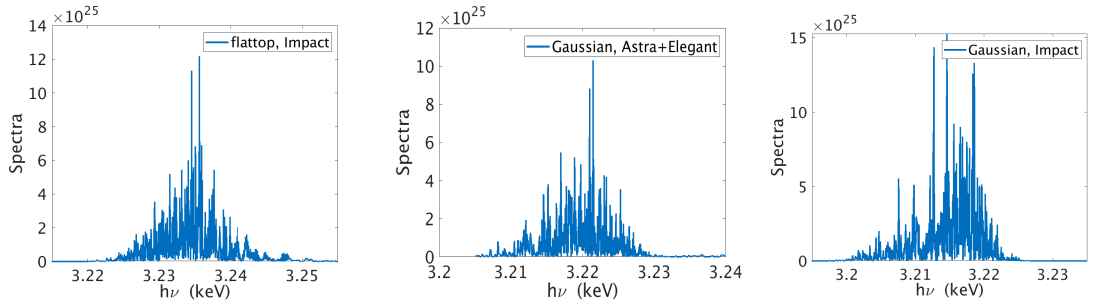


**Figure 12: FEL spectrum at exit of hard x-ray undulator for the three cases as shown in Figure 11.**

Recently, J. Qiang provided a new simulated beam from IMPACT based on a flattop laser. It is achieved using a fast longitudinal phase space optimization method [13], which got a higher core current ~1200A as shown in Figure 13 (it is close to 1100A if not counting the folded low energy particles in the phase space). We performed FEL simulations with this new beam and show the hard x-ray FEL results in Figure 14.

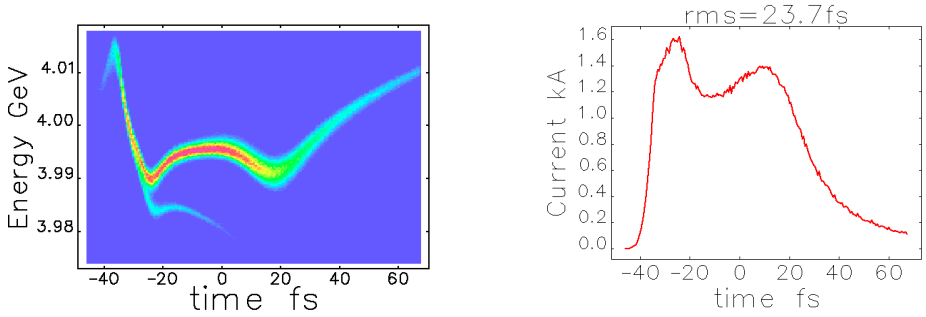


**Figure 13: A new simulated beam from IMPACT based on a flat-top laser, with a higher peak current. Bunch head is to the left.**

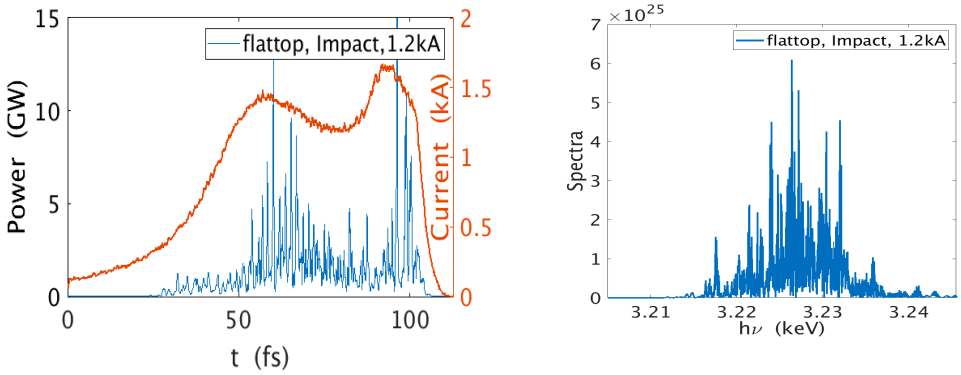


**Figure 14: The FEL power profile and spectrum at the end of the hard x-ray undulator using beam in Figure 13. No taper is applied. On the left figure, the bunch head is to the right.**

We show the gain curves for the four cases (flat-top laser with peak current 800A and 1200A, and Gaussian shape laser with Elegant and IMPACT simulations) in Figure 15. We see the Gaussian case beam has a higher gain than the flattop case, mainly due to the higher beam current in these Gaussian beam configurations. For the Gaussian laser beam, the IMPACT setup has a slightly higher current which leads to higher FEL saturation pulse energy than the Astra + Elegant simulated beam. For the flat-top laser case, the recent new high current 1200-A beam showed better gain than 800-A beam; the gain of the 1200-A beam from flat-top laser is close to but still slightly lower than the Gaussian laser beam, one reason is that the effective core current is actually 1100 A which is smaller than the Gaussian laser case, on the other hand, the configuration is from fast longitudinal optimization, and we think the transverse emittance can be further optimized. These gain curves show that even the injector beam emittance from a Gaussian shape laser is slightly larger than the flattop case, but it can lead to a higher final peak current after compression without current spikes which helps the FEL gain.

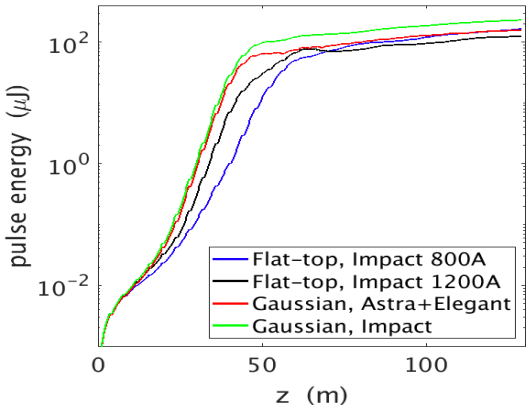


**Figure 15: The FEL gain curves for the four cases shown in Figure 11 and 14. FEL photon energy is 3.25 keV. No post-saturation taper is applied here.**

# 4.4 SXR (1.25 keV) FEL simulations with Genesis

With the beam similar to the one in Figure 7 but tracked through the soft x-ray spreader to the entrance of the soft x-ray undulator, we did one FEL simulation at 1.25 keV. We plot the FEL power profile, spectrum, and the gain curve in Figure 16. For comparison, we also included the gain curve for the beam (~800A peak current) from a flat-top laser (the same reference as used in Figure 6 soft x-ray 1.25 keV case]).

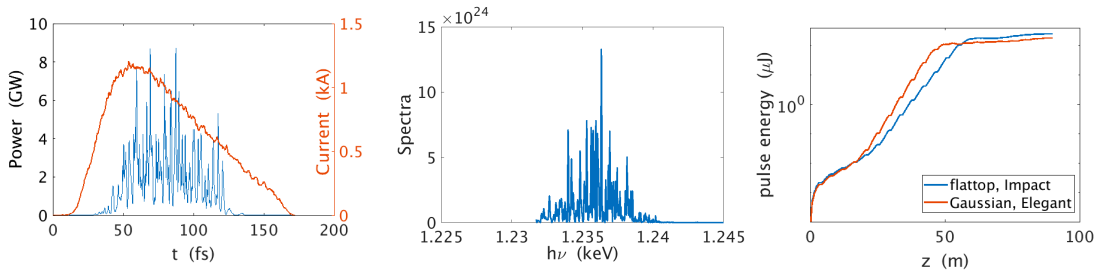


**Figure 16: SXR simulations with the beam from configuration-2, at 1.25 keV. In the gain curve, the flattop case used the flattop laser beam as in Ref. [1], ~800 A.**

# 5 A “Standard” configuration

We set up a “standard” linac and chicane configuration based on a Gaussian shape injector laser, considering both 100 pC and 50 pC case. Here we try to use a same chicane R56 setup for the two bunch charges. The main parameters are listed in Table 5. Note for both cases the injector beam energy is assumed to be 100 MeV.

Based on this standard configuration, we show the final electron beam at the entrance of the undulator in Figure 17 for 100 pC and 50 pC bunch charge, simulated by Astra and Elegant.

**Table 5: A "standard" configuration based on a Gaussian shape injector laser.**

| Parameters | 50 pC | 100 pC | unit |
|---|---|---|---|
| Injector beam E | 100 | 100 | MeV |
| Laser heater | 5 | 7 | keV |
| L1 amplitude | 231 | 231 | MV |
| L1 phase | -25 | -24.9 | deg |
| L1H phase | -170 | -172.5 | deg |
| L1H Amp. | 60 | 60 | MV |
| BC1 Energy | 250 | 250 | MeV |
| BC1 R56 | -53 | -53 | mm |
| L2 amplitude | 1405 | 1479 | MV |
| L2 phase | -27.1 | -32.3 | deg |
| BC2 energy | 1500 | 1500 | MeV |
| BC2 R56 | -45 | -45 | mm |
| L3 amplitude | 2500 | 2500 | MV |
| L3 phase | 0 | 0 | deg |
| final energy | 4000 | 4000 | MeV |

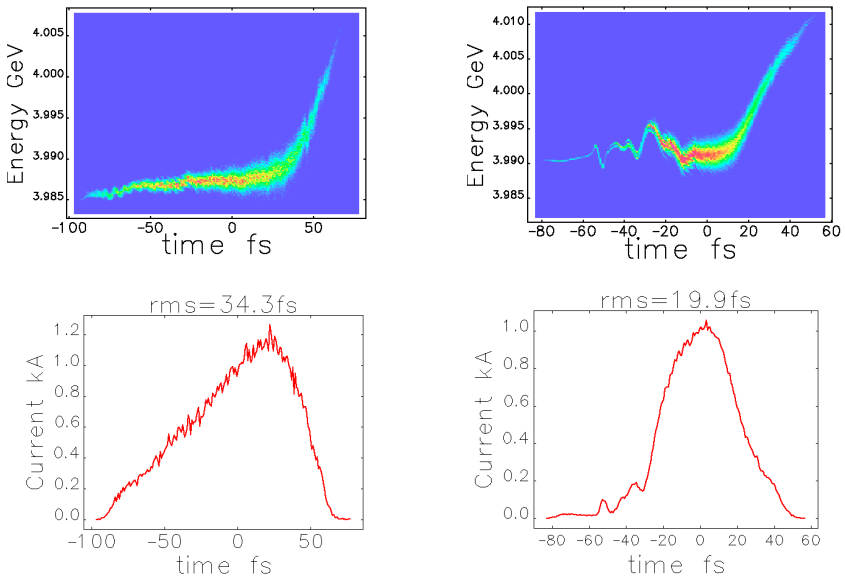


**Figure 17: The electron beam at the hard x-ray undulator entrance based on the "standard" configuration in Table 5. Left: 100 pC; Right: 50 pC. Bunch head is to the left.**

# 6 Conclusions

Using the 100-pC bunch charge as an example, we performed start-to-end simulations using the measured Gaussian shape injector laser to evaluate the beam quality and FEL performance. An IMPACT simulation including the 3-D space charge from the injector to the undulator entrance has been performed to benchmark the microbunching instability concerns. With a higher achievable beam current, the overall FEL performance is not degraded comparing to the cases using flattop injector laser. A standard configuration is proposed considering both 100 pC and 50 pC bunch charge which can be used in the commissioning stage.

# 7 Acknowledgements

We thank D. Cesar for Genesis simulation discussions, and C. Mitchell, F. Zhou and Z. Zhang for injector simulation discussions.

**Reference:**

[1] G. Marcus and J. Qiang, LCLS-II technical note LCLS-II-17-04.

[2] Astra, https://www.desy.de/~mpyflo/

[3] https://journals.aps.org/prab/abstract/10.1103/PhysRevSTAB.8.034202

[4] https://ieeexplore.ieee.org/document/996017

[5] https://github.com/ChristopherMayes/xopt/tree/master/examples/xopt_class

[6] https://github.com/slaclab/lcls-lattice

[7] https://github.com/slaclab/lcls-injector-optimization

[8] M. Borland, "elegant: A Flexible SDDS-Compliant Code for Accelerator Simulation," Advanced. Photon Source LS-287, September 2000.

[9] K. Bane and P. Emma, in Proceedings of the 21st Particle Accelerator Conference, PAC2005, Knoxville, TN, 2005. (IEEE, Piscataway, NJ, 2005), p. 4266.

[10] S. Reiche, Nuclear Instruments and Methods in Physics Research Section A, Volume 429, Issue 1-3, p. 243-248.

[11] J. Qiang, R. D. Ryne, S. Habib, V. Decyk, An object-oriented parallel particle-in-cell code for beamdynamics simulation in linear accelerators, J. Comput. Phys. 163, (2000) p. 434.

[12] J. Qiang, S. Lidia, R. D. Ryne, and C. Limborg-Deprey, A three-dimensional quasi-static model for high brightnees beam dynamics simulation, Phys. Rev. ST Accel. Beams 9, (2006) 044204.

[13] J. Qiang, Fast longitudinal beam dynamics optimization in x-ray free electron laser linear accelerators, Phys. Rev. Accel. Beams 22, 094401.